Research on Graphical Modeling and Low Voltage Ride-Through Strategies of Doubly Fed Induction Generator Based Wind Turbine System

PhD Candidate：Peng Ling
Supervisor：Professor Li Yongdong
Doctor Francois Bruno

June 17, 2010

Defense for the PhD Degree

Outline

- Introduction
- Modeling and control strategies of an energy conversion system
- Graphical modeling and control strategies of a DFIG wind turbine
- Modified vector control strategy of the DFIG against voltage dips
- LVRT performance of the DFIG system with an active crowbar
- Reconfiguration of control strategies for high power DFIG system
- Conclusion and perspective

Outline

- Introduction
- Modeling and control strategies of an energy conversion system
- Graphical modeling and control strategies of a DFIG wind turbine
- Modified vector control strategy of the DFIG against voltage dips
- LVRT performance of the DFIG system with an active crowbar
- Reconfiguration of control strategies for high power DFIG system
- Conclusion and perspective

Introduction

- Context
  - Wind energy
    - Conventional energy source consumption
    - Increasing environmental concern
    - Nonpolluting and economically viable
    - Institutional and governmental support
    - Wind energy potential
    - Improvement of wind technology

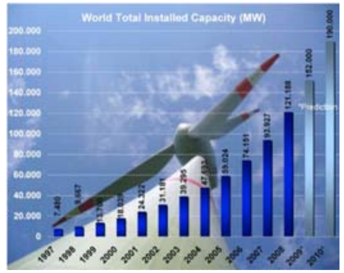

  - Research focus
    - Interaction between wind energy conversion system and network
      - Increase the reliability of wind turbines
      - Improve the adaptability to abnormal grid condition

Introduction

- Wind energy conversion technology development
  - Fixed-pitch fixed-speed wind turbines
    - ↓ Pitch control, increase starting torque, smooth output power
  - Variable pitch fixed-speed wind turbines
    - ↓ Power electronics, improve energy conversion efficiency
  - Variable pitch variable speed wind turbines

- Partial-scale converter

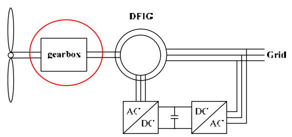

- low cost, high efficiency
- gearbox maintenance

- Full power converter

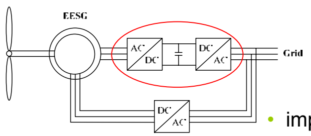

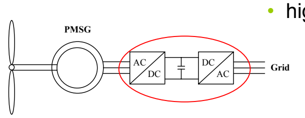

- improved reliability
- high cost, low efficiency

Introduction

- Low voltage ride-through capability
  - LVRT requirement
    - Remain connected during faults
    - Support active and reactive power
    - Resume normal operation fast

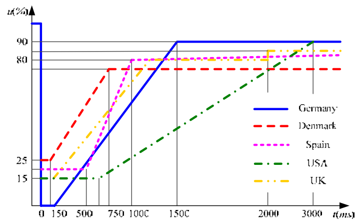

  - Direct-drive system
    - Interfaced by power converter
      - Ride-through of grid side converter

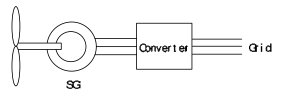

  - DFIG system
    - Direct connection to the gird
      - Large transients of the generator
    - Small capacity power converter
      - Provider partial control of the generator

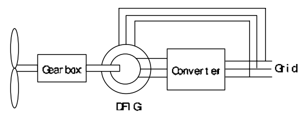

- LVRT strategies of the DFIG system
  - Active method by improving control strategy
    - Improved vector control
    - Direct Power Control
    - Flux Magnitude and Phase Angle control
    - Non-linear control
  - No additional cost
  - Only suitable for small dips
  - Passive scheme with additional hardware device
    - Rotor side
      - Absorb reactive power from gird
    - DC side
      - Cannot reduce rotor over-current
    - Stator side
      - Large dissipation, generator is disconnected
  - for sever dips
  - High cost, complex control

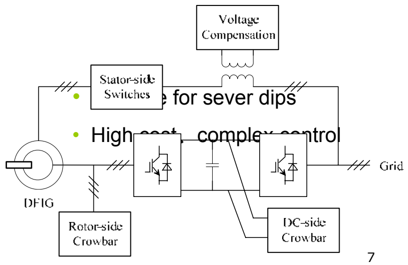

- Main work in the dissertation
  - Modeling and control strategy of the DFIG based wind turbine system
    - Design a process for modeling and controlling a system
    - Obtain the graphical model of the studied system
    - Deduce the control strategies with inversion rules
  - LVRT schemes of the wind turbine based on DFIG
    - Improve the vector control strategy of the DFIG
    - Design a protection scheme by using active crowbar
  - Control strategies of high power DFIG system
    - Design a new current control method for NPC converter
    - Deduce the hierarchical control structure of the studied system

Outline

Different descriptions of a system

- System models
  - Mathematic model
    - Based on equations
    - Priority to the functionality
    - Virtual links between subsystems
    - Application to analysis, control
  - Graphical model
    - Based on graphical elements
    - Priority to the physical structure
    - Physical links between subsystems
    - Application to design

$$\begin{cases} u_1 = ku_2 \\ i_2 = ki_1 \end{cases}$$

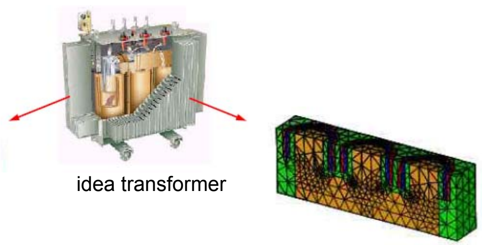

idea transformer

Graphical descriptions

- Different graphical tools
  - Bond Graph (USA)
    - Action and reaction principle
    - Derivative causality problem
  - Power-Oriented Graphs (Italy)
    - Correspond to transfer function
    - Derivative causality problem
  - Power Flow Diagram(Germany)
    - Integral causality
    - Efficiency study
  - Energetic Puzzles (LAPLACE, France)
    - Energy conversion

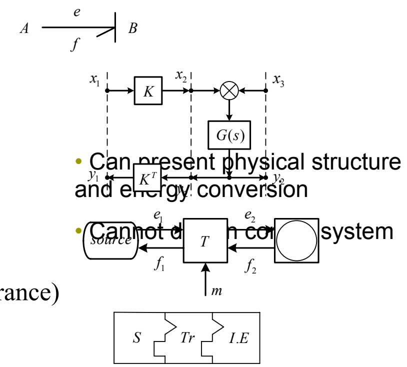

- Causal Ordering Graph
- Energetic Macroscopic Representation

} (L2EP, France)

Causal Ordering Graph

- A tool for system modeling and control law synthesis
  - Physical causality is integral

Static relation
- Time independence
- External causality
- Algebraic equation

Dynamic relation
- Time dependence
- Internal causality
- Differential equation

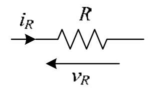

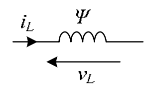

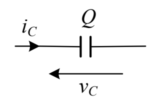

$R_{R1}:\ v_R(t)=r\,i_R(t)$ $R_{R2}:\ i_R(t)=\frac{1}{r}v_R(t)$ $R_L:\ v_L(t)=\frac{d\psi(t)}{dt}=L\frac{di_L(t)}{dt}$ $R_C:\ i_C(t)=\frac{dQ(t)}{dt}=C\frac{dv_C(t)}{dt}$

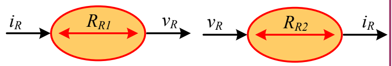

Causal Ordering Graph

- Inversion based control methodology
  - Principle of the inversion based control

Static relation
- direct inversion

$R_a:\ y(t)=R_a(x(t))$

$R_{ac}: x_{reg}(t)=R_{ac}(y_{ref}(t))$

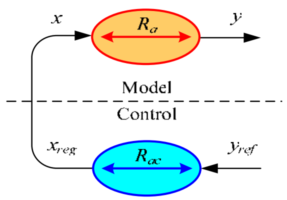

Dynamic relation
- indirect inversion

$R_b:\ y(t)=R_b(x(t))$

$R_{bc}: x_{reg}(t)=C_{PI}(y_{ref}(t)-\tilde{y}(t))$

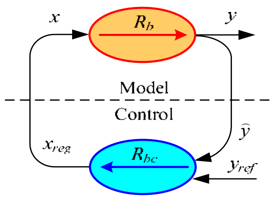

Energetic Macroscopic Representation

- A synthetic description of the overall system
  - Action-reaction principle, integral causality

Source

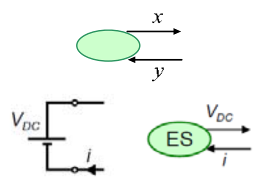

Accumulation

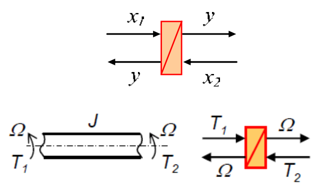

Converter
- electrical
- mechanical

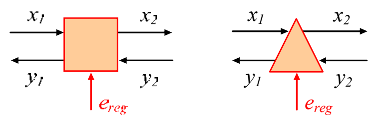

- electromechanical

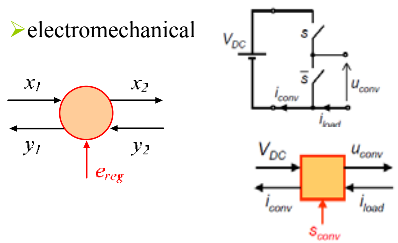

Energetic Macroscopic Representation

- Coupling
  - electrical

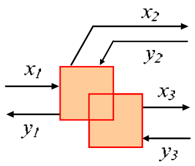

  - electromechanical

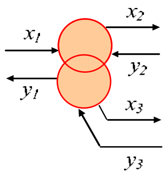

  - mechanical

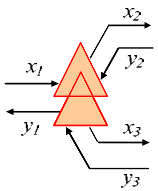

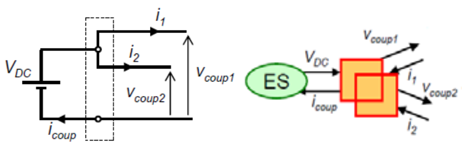

Energetic Macroscopic Representation

- Maximal Control Structure
  - A maximum of control operations and measurements
  - Assume that all variables are measurable
  - Specific inversion rules
    - direct inversion

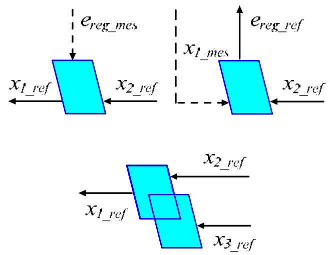

    - indirect inversion

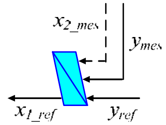

    - control strategy

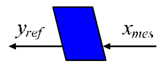

Modeling and control strategy of a system

- Process for modeling and controlling an energy conversion system

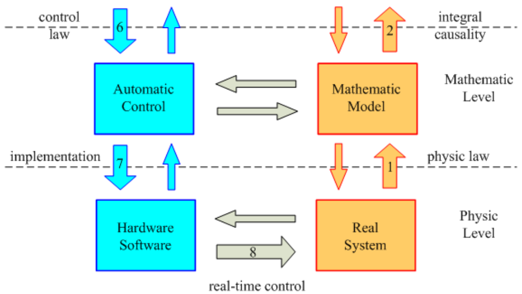

- graphical tools
- traditional method

Outline

- Introduction
- Modeling and control strategies of an energy conversion system
- Graphical modeling and control strategies of a DFIG wind turbine
- Modified vector control strategy of the DFIG against voltage dips
- LVRT performance of the DFIG system with an active crowbar
- Reconfiguration of control strategies for high power DFIG system
- Conclusion and perspective

Modeling of the DFIG wind turbine system

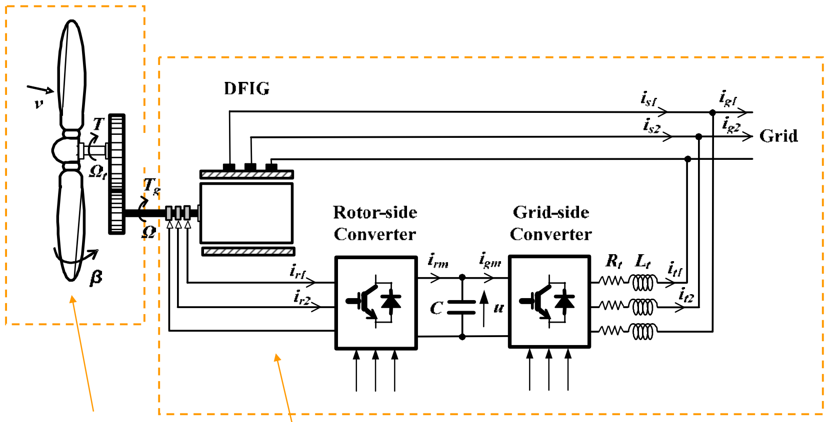

- Mechanical parts
  - turbine
  - shaft
  - gearbox
- Electrical parts
  - DFIG, power converters, DC bus, filter

Modeling of the DFIG wind turbine system

- Modeling of the turbine

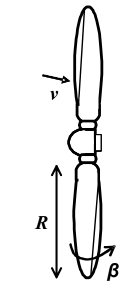

R_1: $T = \dfrac{P}{\Omega_t} = \dfrac{1}{2} C_p \rho S v^3 \dfrac{1}{\Omega_t}$

R_3: $C_p(\lambda,\beta) = (0.5 - 0.167(\beta-2))\sin[\dfrac{\pi(\lambda+0.1)}{18.5-0.3(\beta-2)}] - 0.00184(\lambda-3)(\beta-2)$

R_2: $\lambda = \dfrac{R\Omega_t}{v}$

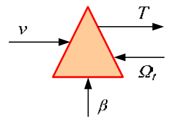

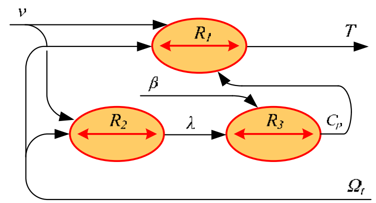

Modeling of the DFIG wind turbine system

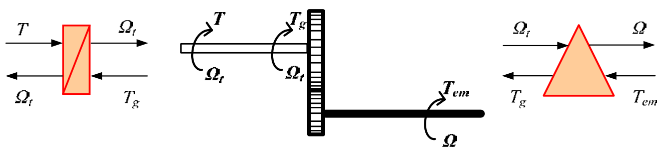

- Modeling of the shaft

$$\begin{cases} R_4:\ J\dfrac{d\Omega_t}{dt} = T_t \\ R_5:\ T_t = T - T_g - T_{vis} \\ R_6:\ T_{vis} = f\Omega_t \end{cases}$$

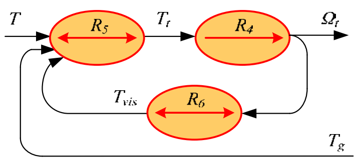

- Modeling of the gearbox

$$\begin{cases} R_7:\ \Omega = G\Omega_t \\ R_8:\ T_g = GT_{em} \end{cases}$$

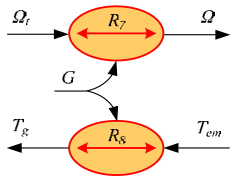

Modeling of the DFIG wind turbine system

- Modeling of the DFIG
  - voltage equations

R_9: $\dfrac{d\psi_{sd}}{dt} = v_{sd} - R_s i_{sd} + \omega_s \psi_{sq}$ $\quad$ R_{11}: $\dfrac{d\psi_{rd}}{dt} = v_{rd} - R_r i_{rd} + \omega_r \psi_{rq}$

R_{10}: $\dfrac{d\psi_{sq}}{dt} = v_{sq} - R_s i_{sq} - \omega_s \psi_{sd}$ $\quad$ R_{12}: $\dfrac{d\psi_{rq}}{dt} = v_{rq} - R_r i_{rq} - \omega_r \psi_{rd}$

  - flux equations

R_{13}: $\begin{bmatrix} i_{sd} \\ i_{rd} \end{bmatrix} = \begin{bmatrix} L_s & M \\ M & L_r \end{bmatrix}^{-1} \begin{bmatrix} \psi_{sd} \\ \psi_{rd} \end{bmatrix}$ $\quad$ R_{14}: $\begin{bmatrix} i_{sq} \\ i_{rq} \end{bmatrix} = \begin{bmatrix} L_s & M \\ M & L_r \end{bmatrix}^{-1} \begin{bmatrix} \psi_{sq} \\ \psi_{rq} \end{bmatrix}$

  - speed equation

R_{15}: $\omega_r = \omega_s - p\Omega$

  - torque equation

R_{16}: $T_{em} = p(\psi_{sd} i_{sq} - \psi_{sq} i_{sd})$

Modeling of the DFIG

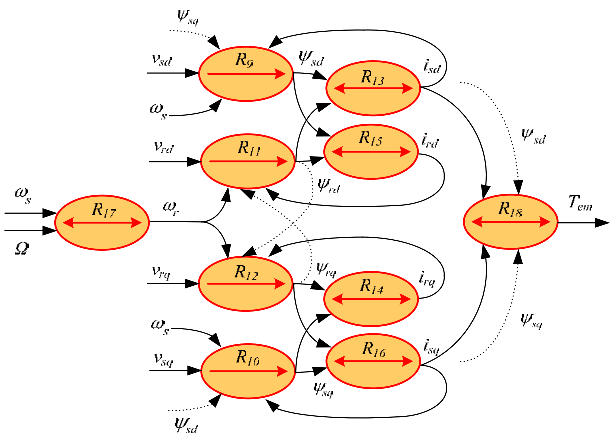

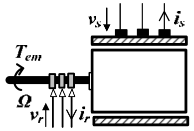

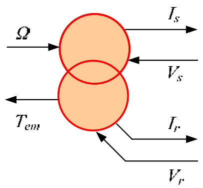

Modeling of the power converters

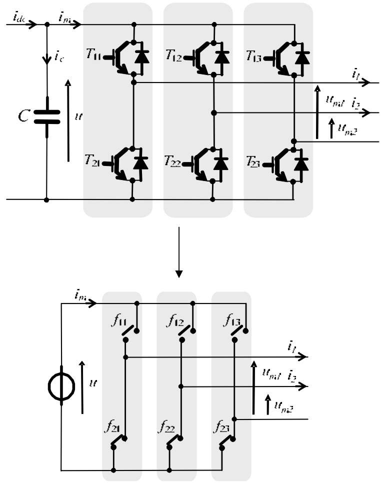

- switching function

$$s_{ij} \in \{0,1\}, \text{ with } \begin{cases} i \in \{1,2,3\} \\ j \in \{1,2\} \end{cases}$$

- modulation function

$$m = \begin{bmatrix} m_1 \\ m_2 \end{bmatrix} = \begin{bmatrix} 1 & 0 & -1 \\ 0 & 1 & -1 \end{bmatrix} \begin{bmatrix} s_{11} \\ s_{12} \\ s_{13} \end{bmatrix}$$

- mathematic model

$$\begin{cases} u_m = \begin{bmatrix} u_{m1} \\ u_{m2} \end{bmatrix} = mu \qquad v_m = \frac{1}{3}\begin{bmatrix} 2 & -1 \\ -1 & 2 \end{bmatrix} u_m \\ i_m = m^T \begin{bmatrix} i_1 \\ i_2 \end{bmatrix} = m^T i \end{cases}$$

Modeling of the power converters

- rotor side converter

$$\begin{cases} R_{17}:\ m_r = \begin{bmatrix} 1 & 0 & -1 \\ 0 & 1 & -1 \end{bmatrix} s_r \\ R_{18}:\ u_r = m_r u \\ R_{19}:\ i_{rm} = m_r^{\ T} i_r \\ R_{20}:\ v_r = \frac{1}{3}\begin{bmatrix} 2 & -1 \\ -1 & 2 \end{bmatrix} u_r \end{cases}$$

- grid side converter

$$\begin{cases} R_{21}:\ m_g = \begin{bmatrix} 1 & 0 & -1 \\ 0 & 1 & -1 \end{bmatrix} s_g \\ R_{22}:\ u_t = m_g u \\ R_{23}:\ i_{gm} = m_g^{\ T} i_t \\ R_{24}:\ v_t = \frac{1}{3}\begin{bmatrix} 2 & -1 \\ -1 & 2 \end{bmatrix} u_t \end{cases}$$

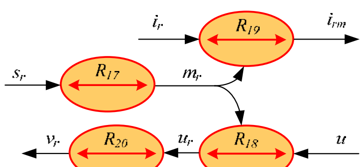

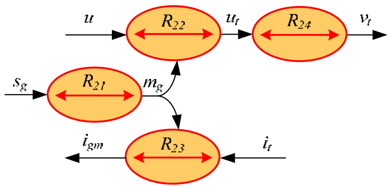

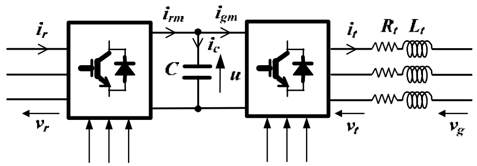

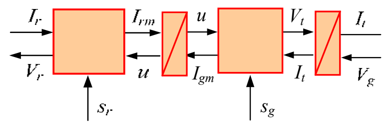

Modeling of the filter

$$\begin{cases} R_{27}:\ L_t \frac{di_t}{dt} = v_f \\ R_{28}:\ v_f = v_t - v_r - v_g \\ R_{29}:\ v_r = R_t i_t \end{cases}$$

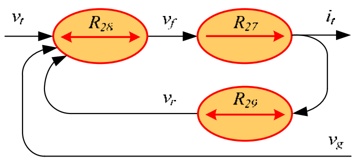

Modeling of the DC bus

$$\begin{cases} R_{25}:\ C\frac{du}{dt} = i_c \\ R_{26}:\ i_c = i_{rm} - i_{gm} \end{cases}$$

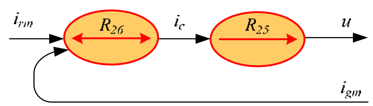

- Energetic Macroscopic Representation
- Maximum Control Structure

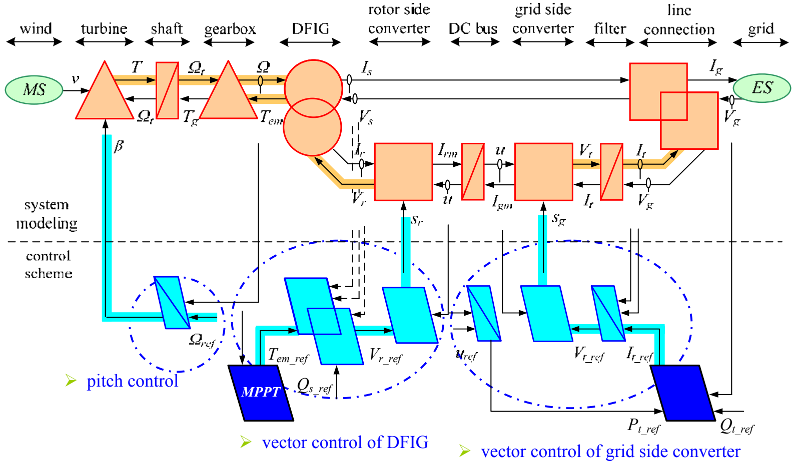

- Vector control of the DFIG $\psi_{sd} = \psi_s$

R_{r1}: $\frac{di_{rd}}{dt} = \frac{1}{\sigma L_r}(v_d - R_r i_{rd})$

R_{r2}: $\frac{di_{rq}}{dt} = \frac{1}{\sigma L_r}(v_q - R_r i_{rq})$

R_{r3}: $v_d = v_{rd} - e_q$

R_{r4}: $v_q = v_{rq} - e_d - e_\psi$

R_{r5}: $e_d = \sigma L_r \omega_r i_{rd}$

R_{r6}: $e_q = -\sigma L_r \omega_r i_{rq}$

R_{r7}: $e_\psi = \frac{M}{L_s}\omega_r \psi_s$

R_{r8}: $T_{em} = p\psi_{sd} i_{sq} = -p\psi_s \frac{M}{L_s} i_{rq}$

R_{r9}: $Q_s = v_{sq} i_{sd} = \frac{v_s \psi_s}{L_s} - \frac{v_s M}{L_s} i_{rd}$

R_{r1c}: $v_{d\_ref} = C_{PI}(i_{rd\_ref} - \hat{i}_{rd})$

R_{r2c}: $v_{q\_ref} = C_{PI}(i_{rq\_ref} - \hat{i}_{rq})$

R_{r3c}: $v_{rd\_ref} = v_{d\_ref} + e_{q\_ref}$

R_{r4c}: $v_{rq\_ref} = v_{q\_ref} + e_{d\_ref} + e_{\psi\_ref}$

R_{r5c}: $e_{d\_ref} = \sigma L_r \omega_r \hat{i}_{rd}$

R_{r6c}: $e_{q\_ref} = -\sigma L_r \omega_r \hat{i}_{rq}$

R_{r7c}: $e_{\psi\_ref} = \frac{M}{L_s}\omega_r \tilde{\psi}_s$

R_{r8c}: $i_{rq\_ref} = -\frac{1}{p\psi_{s\_ref}}\frac{L_s}{M} T_{em\_ref}$

R_{r9c}: $i_{rd\_ref} = \frac{\psi_{s\_ref}}{M} - \frac{L_s}{v_{s\_ref} M} Q_{s\_ref}$

- Vector control of the DFIG

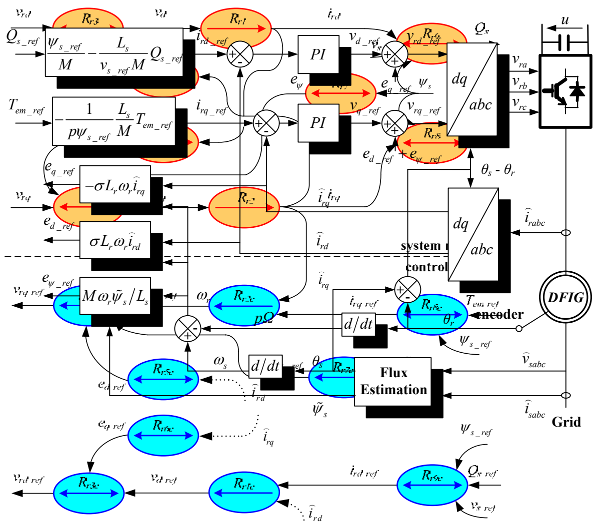

- Vector control of the grid side converter $v_{gd} = v_g$

R_{g1}: $v_{td} = v_d - e_q + v_g$

R_{g2}: $v_{tq} = v_q - e_d$

R_{g3}: $\frac{di_{td}}{dt} = \frac{1}{L_t}(v_d - R_t i_{td})$

R_{g4}: $\frac{di_{tq}}{dt} = \frac{1}{L_t}(v_d - R_t i_{tq})$

R_{g5}: $e_d = -L_t \omega_s i_{td}$

R_{g6}: $e_q = L_t \omega_s i_{tq}$

R_{g7}: $P_t = v_g i_{td}$

R_{g8}: $Q_t = -v_g i_{tq}$

R_{g1c}: $v_{td\_ref} = v_{d\_ref} - e_{q\_ref} + \hat{v}_g$

R_{g2c}: $v_{tq\_ref} = v_{q\_ref} - e_{d\_ref}$

R_{g3c}: $v_{d\_ref} = C_{PI}(i_{td\_ref} - \hat{i}_{td})$

R_{g4c}: $v_{q\_ref} = C_{PI}(i_{tq\_ref} - \hat{i}_{tq})$

R_{g5c}: $e_{d\_ref} = -L_t \omega_s \hat{i}_{td}$

R_{g6c}: $e_{q\_ref} = L_t \omega_s \hat{i}_{tq}$

R_{g7c}: $i_{td\_ref} = \frac{P_{t\_ref}}{\hat{v}_g}$

R_{g8c}: $i_{tq\_ref} = -\frac{Q_{t\_ref}}{\hat{v}_g}$

Control strategy of the system

- Vector control of the grid side converter

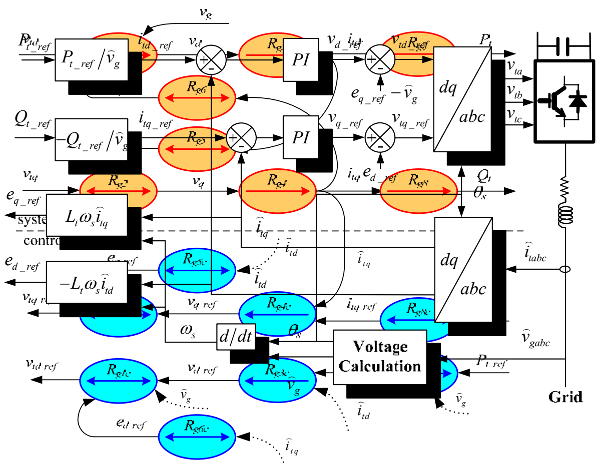

Control strategy of the system

- Control of the DC-link voltage

$R_{c1}: \; C\frac{du}{dt} = i_c$

$R_{c1c}: \; i_{c\_ref} = C_{PI}(u_{ref} - \hat{u})$

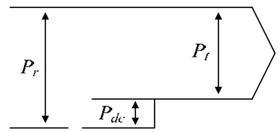

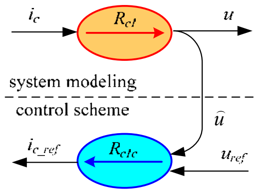

$R_{e1}: \; P_r = u i_c + P_t$

$R_{e1c}: \; P_{t\_ref} = \tilde{P}_r - \tilde{u} i_{c\_ref}$

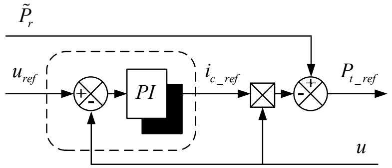

Modeling and control strategy of the system

- Simulation results
  - Decoupled control of active and reactive power

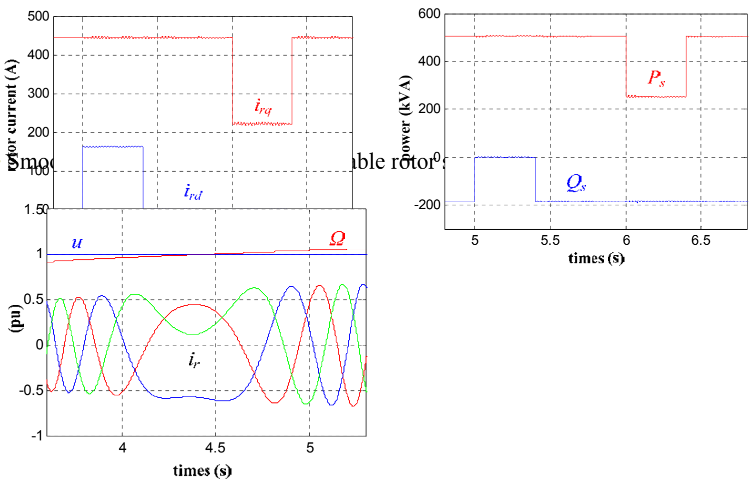

Modeling and control strategy of the system

- Experimental results
  - Activation of grid-side converter
  - Synchronization of DFIG

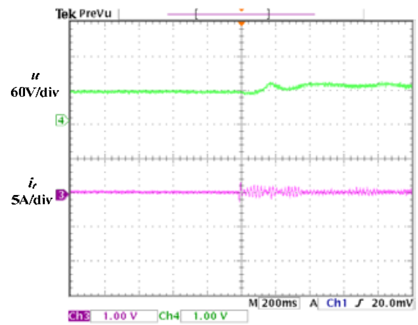

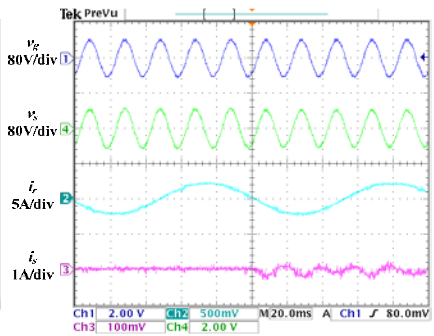

Modeling and control strategy of the system

- Experimental results
  - Steady operation after synchronization
  - MPPT control

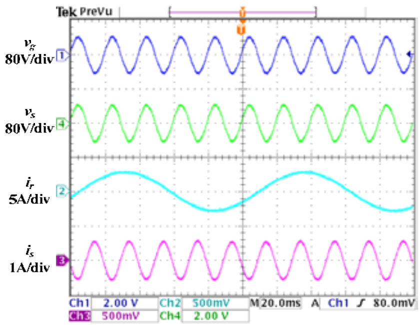

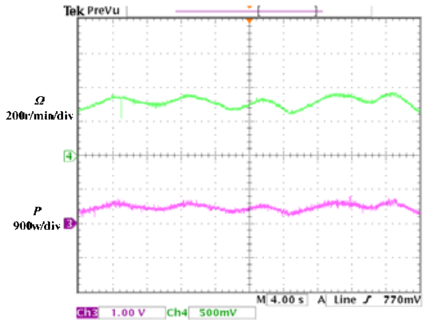

Modeling and control strategy of the system

- Experimental results
  - Decoupled control of active and reactive power
    - active power change
    - reactive power change

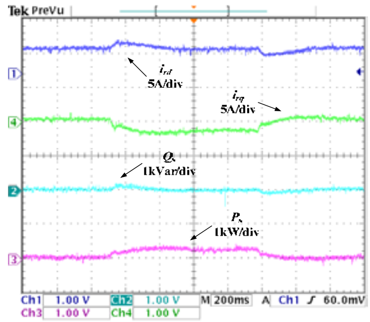

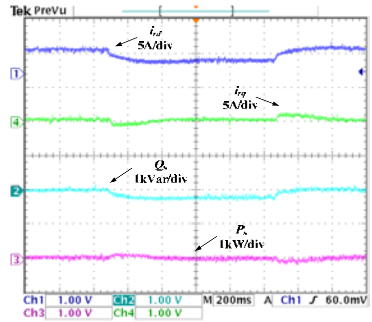

Modeling and control strategy of the system

- Experimental results
  - Variable speed constant frequency operation
    - acceleration
    - deceleration

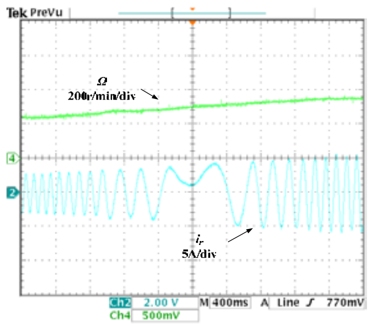

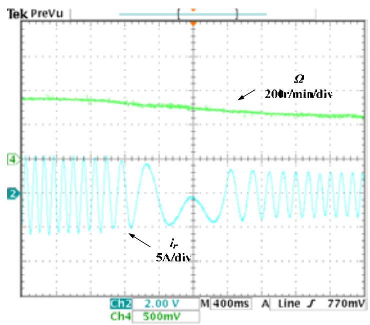

Outline

- Introduction
- Modeling and control strategies of an energy conversion system
- Graphical modeling and control strategies of a DFIG wind turbine
- Modified vector control strategy of the DFIG against voltage dips
- LVRT performance of the DFIG system with an active crowbar
- Reconfiguration of control strategies for high power DFIG system
- Conclusion and perspective

- Voltage dip
  - A sudden reduction (between 10% and 90%) of the voltage at a point in the electrical system, which lasts for an half of a cycle to 1 min
    - magnitude, duration, phase-angle jump

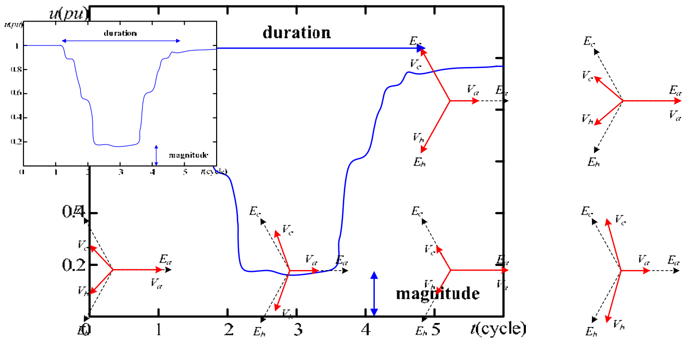

- Dynamic behavior of the system during voltage dips

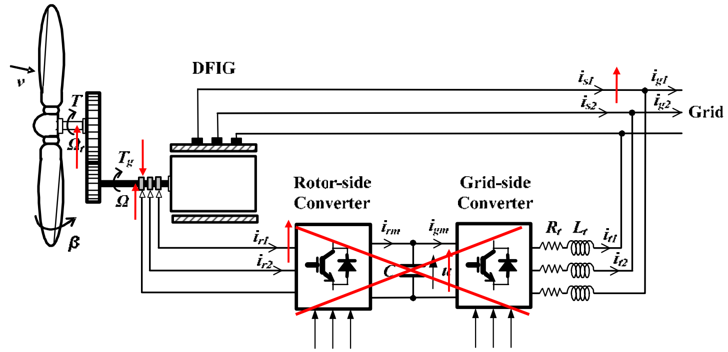

- LVRT requirements
  - Prevent over-current and over-voltage
  - Prevent over-speed and reduce mechanical impulse
  - Resume normal operation fast after grid voltage recovers

- Stator flux analysis

$$\vec{v}_s = R_s\vec{i}_s + \frac{d\vec{\psi}_s}{dt} \qquad \vec{v}_s(t) = \begin{cases} V_1 e^{j\omega_s t}(t < t_0) \\ V_2 e^{j\omega_s t}(t \ge t_0) \end{cases}$$

$$\vec{\psi}_s(t) = \begin{cases} \vec{\psi}_{sf1}(t)(t < t_0) \\ \vec{\psi}_{sf2}(t) + \vec{\psi}_{sn}(t)(t \ge t_0) \end{cases}$$

$$\vec{\psi}_{sf2}(t) = \frac{V_2}{j\omega_s} e^{j\omega_s t}$$ forced flux

$$\vec{\psi}_{sn}(t) = \frac{V_1 - V_2}{j\omega_s} e^{-\frac{t}{\tau}}$$ natural flux

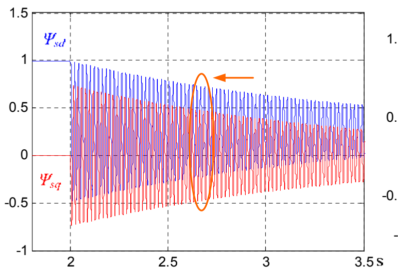

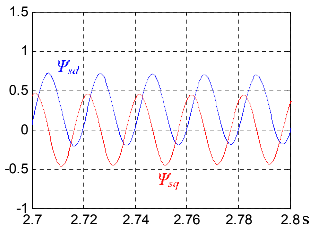

- Conventional vector control strategy

$$\psi_{sd} = \psi_s = \text{constant} \qquad \psi_{sq} = 0 \quad \longrightarrow \quad \frac{d\psi_{sd}}{dt} = 0 \qquad \frac{d\psi_{sq}}{dt} = 0$$

- model

R_{r1}: $\frac{di_{rd}}{dt} = \frac{1}{\sigma L_r}(v_d - R_r i_{rd})$

R_{r2}: $\frac{di_{rq}}{dt} = \frac{1}{\sigma L_r}(v_q - R_r i_{rq})$

R_{r3}: $v_d = v_{rd} + \sigma L_r \omega_r i_{rq}$

R_{r4}: $v_q = v_{rq} - \sigma L_r \omega_r i_{rd} - \frac{M}{L_s}\omega_r \psi_s$

- control

R_{r1c}: $v_{d\_ref} = C_{PI}(i_{rd\_ref} - \hat{i}_{rd})$

R_{r2c}: $v_{q\_ref} = C_{PI}(i_{rq\_ref} - \hat{i}_{rq})$

R_{r3c}: $v_{rd\_ref} = v_{d\_ref} - \sigma L_r \omega_r \hat{i}_{rq}$

R_{r4c}: $v_{rq\_ref} = v_{q\_ref} + \sigma L_r \omega_r \hat{i}_{rd} + \frac{M}{L_s}\omega_r \tilde{\psi}_s$

Modified vector control strategy

$$\psi_{sd} = \tilde{\psi}_{sd} \neq \text{constant} \quad \rightarrow \quad \frac{d\psi_{sd}}{dt} \neq 0$$

$$\psi_{sq} = \tilde{\psi}_{sq} \neq 0 \quad \rightarrow \quad \frac{d\psi_{sq}}{dt} \neq 0$$

model

$$R_{m1}:\ \frac{di_{rd}}{dt} = \frac{1}{\sigma L_r}(v_d - R_r i_{rd})$$

$$R_{m2}:\ \frac{di_{rq}}{dt} = \frac{1}{\sigma L_r}(v_q - R_r i_{rq})$$

$$R_{m3}:\ v_d = v_{rd} + \sigma L_r \omega_r i_{rq} + \frac{M}{L_s}\left(\omega_r \psi_{sq} - \frac{d\psi_{sd}}{dt}\right)$$

$$R_{m4}:\ v_q = v_{rq} - \sigma L_r \omega_r i_{rd} - \frac{M}{L_s}\left(\omega_r \psi_{sd} + \frac{d\psi_{sq}}{dt}\right)$$

$$R_{m5}:\ v_{sd} = \frac{R_s}{L_s}\psi_{sd} - \frac{R_s}{L_s} i_{rd} + \frac{d\psi_{sd}}{dt}$$

$$R_{m6}:\ v_{sq} = \frac{R_s}{L_s}\psi_{sq} - \frac{R_s}{L_s} i_{rq} + \frac{d\psi_{sq}}{dt}$$

control

$$R_{m1c}:\ v_{d\_ref} = C_{PI}(i_{rd\_ref} - \hat{i}_{rd})$$

$$R_{m2c}:\ v_{q\_ref} = C_{PI}(i_{rq\_ref} - \hat{i}_{rq})$$

$$R_{m3c}:\ v_{rd\_ref} = v_{d\_ref} - \sigma L_r \omega_r \hat{i}_{rq} - \frac{M}{L_s}\left(\omega_r \tilde{\psi}_{sq} - \frac{d\psi_{sd}}{dt}_{est}\right)$$

$$R_{m4c}:\ v_{rq\_ref} = v_{q\_ref} + \sigma L_r \omega_r \hat{i}_{rd} + \frac{M}{L_s}\left(\omega_r \tilde{\psi}_{sd} + \frac{d\psi_{sq}}{dt}_{est}\right)$$

$$R_{m5c}:\ \frac{d\psi_{sd}}{dt}_{est} = \hat{v}_{sd} - \frac{R_s}{L_s}\tilde{\psi}_{sd} + \frac{R_s}{L_s}\hat{i}_{rd}$$

$$R_{m6c}:\ \frac{d\psi_{sq}}{dt}_{est} = \hat{v}_{sq} - \frac{R_s}{L_s}\tilde{\psi}_{sq} + \frac{R_s}{L_s}\hat{i}_{rq}$$

Modified vector control strategy

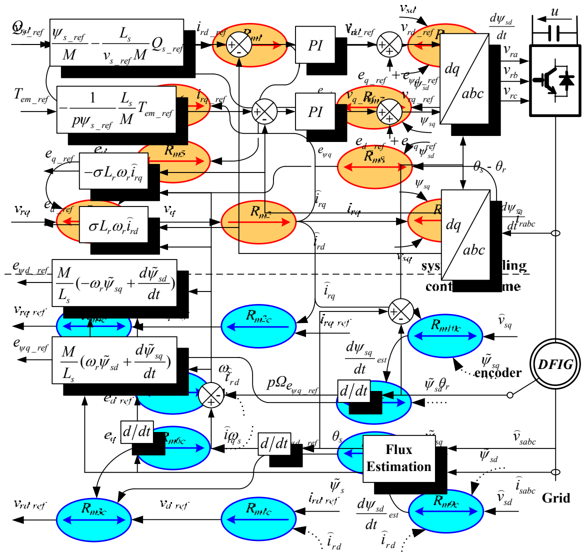

Simulation results (200 ms 33% voltage dip)

(red: modified vector control strategy; blue: conventional vector control strategy)

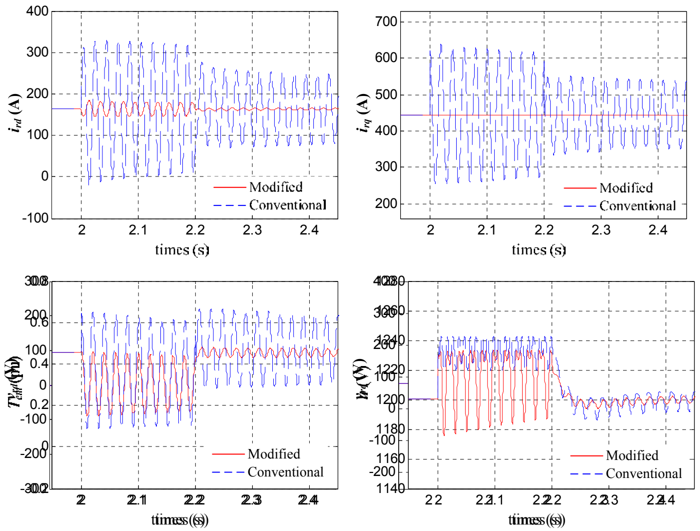

Simulation results (200 ms 33% voltage dip)

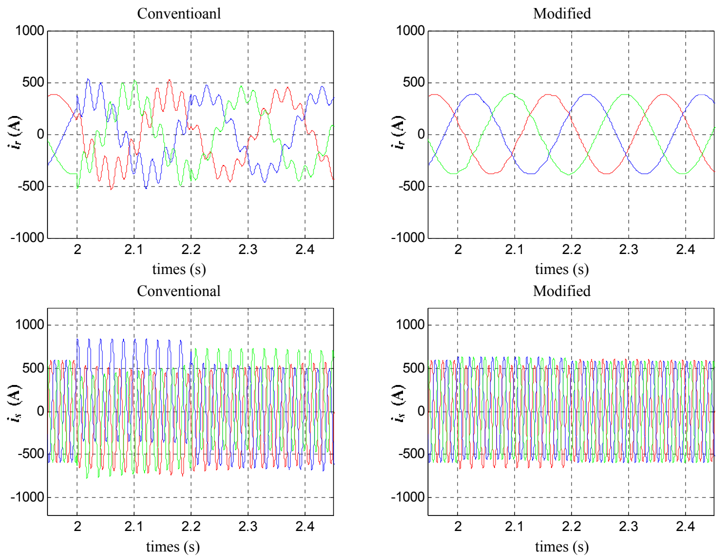

Modified vector control strategy of the DFIG

- Experimental results (500 ms 33% voltage dip)
  - stator flux
  - rotor current

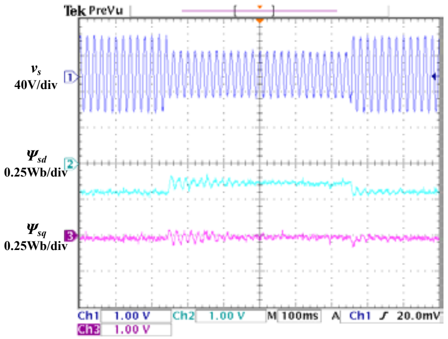

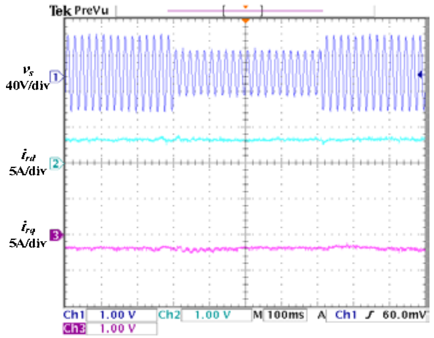

Modified vector control strategy of the DFIG

- Experimental results (500 ms 33% voltage dip)
  - stator and rotor current
  - active and reactive power

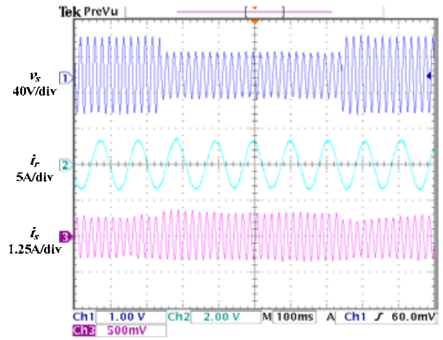

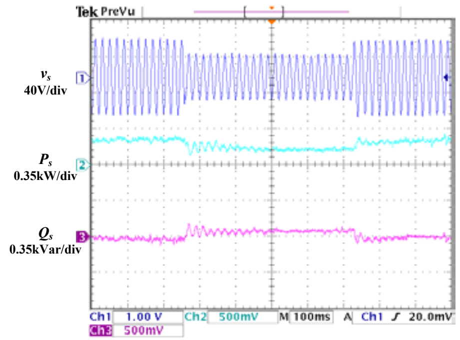

Modified vector control strategy of the DFIG

- Feasibility region of modified vector control strategy
  - Restricted by partial rating power converters
  - Mainly affected by the severity of the fault and the generator speed (slip)

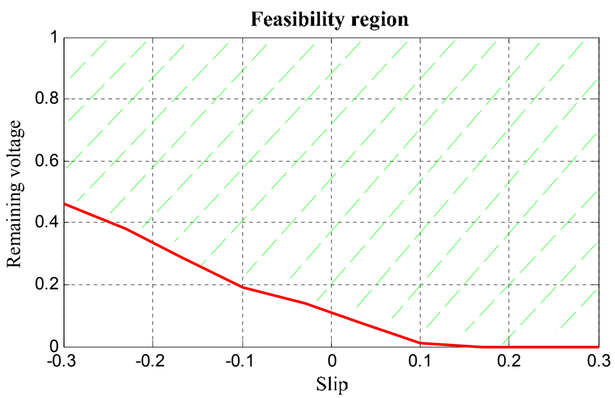

Outline

- Introduction
- Modeling and control strategies of an energy conversion system
- Graphical modeling and control strategies of a DFIG wind turbine
- Modified vector control strategy of the DFIG against voltage dips
- LVRT performance of the DFIG system with an active crowbar
- Reconfiguration of control strategies for high power DFIG system
- Conclusion and perspective

Protection scheme based on active crowbar

- Crowbar circuits
  - Conventional crowbar **turn-off problem**

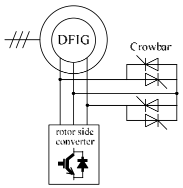

antiparallel thyristor

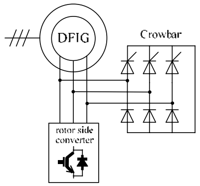

half controlled thyristor bridge

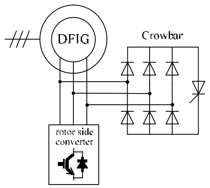

diode bridge and thyristor

  - Active crowbar

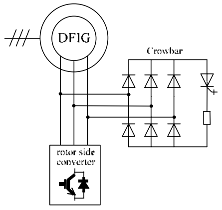

diode bridge and GTO

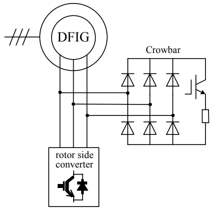

diode bridge and IGBT

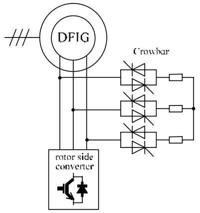

bidirectional switches

Protection scheme based on active crowbar

- Modeling of the active crowbar

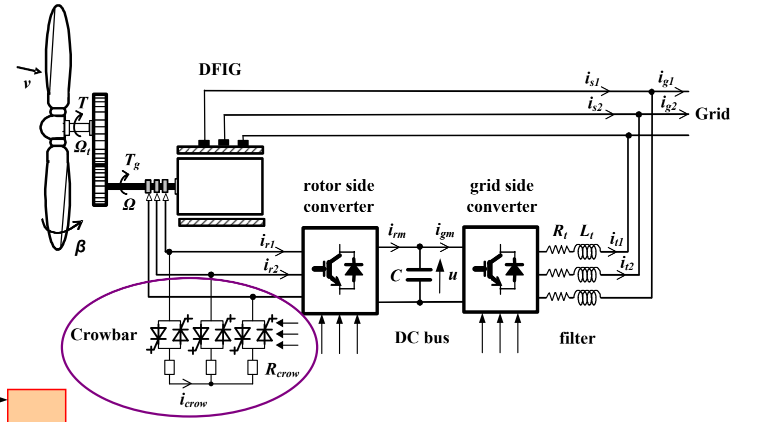

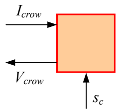

R_{32}: $v_{crow} = s_c R_{crow} i_{crow}$ $\quad s_c = \begin{cases} 1 & \text{switches are closed} \\ 0 & \text{switches are open} \end{cases}$

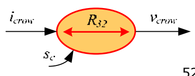

Protection scheme based on active crowbar

- Drawback of crowbar protection
  - Lost of the controllability of the DFIG when the crowbar is triggered
  - The DFIG then behaves as a classical squirrel cage induction machine and absorbs reactive power

- Hysteresis control of the crowbar
  - Reduce the activated time

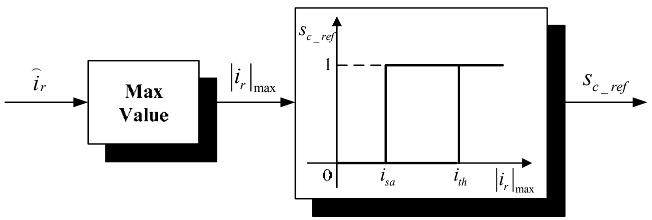

Protection scheme based on active crowbar

- Demagnetization of the DFIG
  - Transient stator flux during the voltage dip

$$\vec{\psi}_s = \vec{\psi}_{sf} + \vec{\psi}_{sn}$$

  - Demagnetization method
    - closed-loop control of the stator flux

$$i_{rd\_ref} = C_{PI}[\psi_{sd\_ref} - \tilde{\psi}_{sd}] \qquad \psi_{sd\_ref} = \psi_{sfd} = \frac{V_2}{\omega_s}$$

$$\longrightarrow$$

$$i_{rq\_ref} = C_{PI}[\psi_{sq\_ref} - \tilde{\psi}_{sq}] \qquad \psi_{sq\_ref} = \psi_{sfq} = 0$$

- Voltage support by the grid side converter

$$Q_{t\_ref} = \sqrt{S_t^2 - P_{t\_ref}^2}$$

Protection scheme based on active crowbar

➢ Synthetic LVRT scheme with the active crowbar

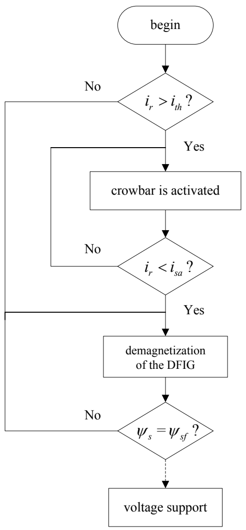

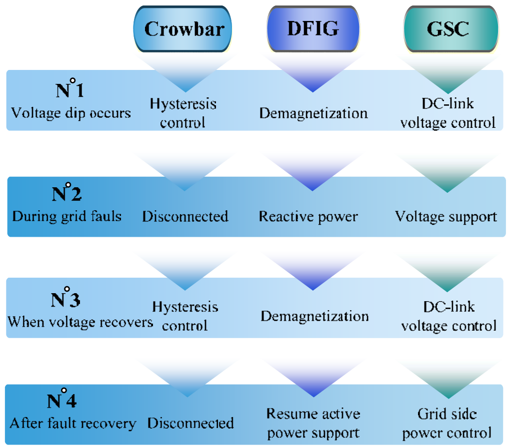

Protection scheme based on active crowbar

➢ Simulation results (0.5 s 85% voltage dip, rated power)

- stator voltage
- crowbar trigger signal

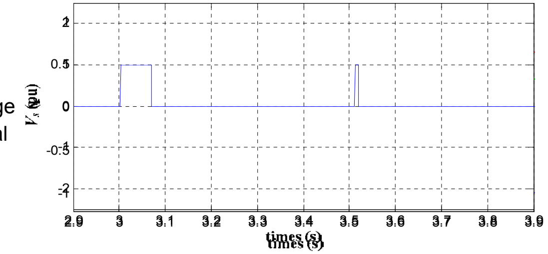

- rotor current

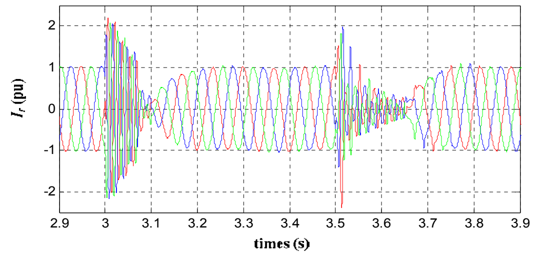

Protection scheme based on active crowbar

➢ Simulation results (0.5 s 85% voltage dip, rated power)

- DC-link voltage
- reactive voltage of DFIG

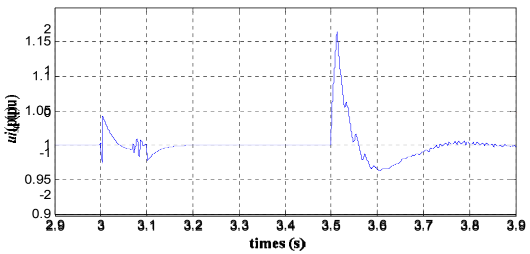

- reactive current of GSC

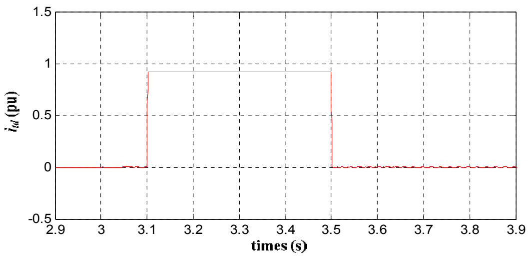

Outline

➢ Introduction

➢ Modeling and control strategies of an energy conversion system

➢ Graphical modeling and control strategies of a DFIG wind turbine

➢ Modified vector control strategy of the DFIG against voltage dips

➢ LVRT performance of the DFIG system with an active crowbar

➢ Reconfiguration of control strategies for high power DFIG system

➢ Conclusion and perspective

- Trend of wind power generation
  - Off-shore application
  - Increase the size and the power rating

REpower 5M

- High power wind turbine system
  - Multilevel converters
    - Realistic alternative to conventional converters

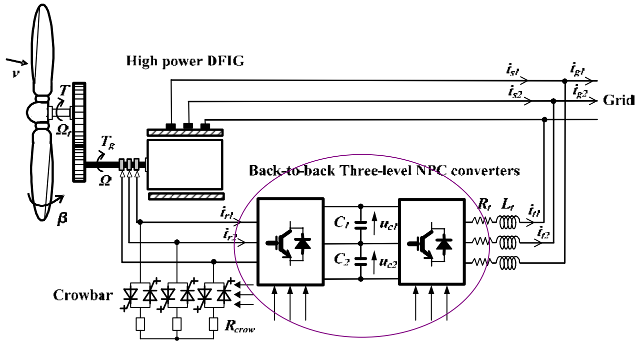

- Modeling of the three-level NPC converters

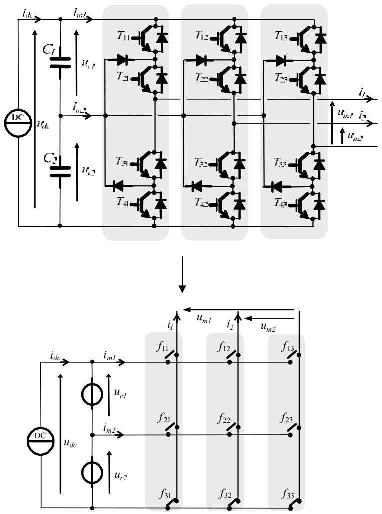

- Switching function

$$s_{ij} \in \{0,1\}, \text{ with} \begin{cases} i \in \{1,2,3\} \\ j \in \{1,2,3\} \end{cases}$$

- Modulation function

$$m = \begin{bmatrix} m_{11} & m_{12} \\ m_{21} & m_{22} \end{bmatrix} = \begin{bmatrix} 1 & 0 & -1 \\ 0 & 1 & -1 \end{bmatrix} \begin{bmatrix} s_{11} & s_{21} \\ s_{12} & s_{22} \\ s_{13} & s_{23} \end{bmatrix}$$

- Mathematic model

$$u_m = \begin{bmatrix} u_{m1} \\ u_{m2} \end{bmatrix} = m \begin{bmatrix} u_{c1} + u_{c2} \\ u_{c2} \end{bmatrix} = mu \qquad v_m = \frac{1}{3}\begin{bmatrix} 2 & -1 \\ -1 & 2 \end{bmatrix} u_m$$

$$i_m = \begin{bmatrix} i_{m1} \\ i_{m2} \end{bmatrix} = m^T \begin{bmatrix} i_1 \\ i_2 \end{bmatrix} = m^T i$$

- Modeling of the three-level NPC converters
  - Rotor side converter

$$\begin{cases} R_1:\ m_r = \begin{bmatrix} 1 & 0 & -1 \\ 0 & 1 & -1 \end{bmatrix} s_r \\ R_2:\ u_r = m_r u \\ R_3:\ i_{rm} = m_r{}^T i_r \\ R_4:\ v_r = \frac{1}{3}\begin{bmatrix} 2 & -1 \\ -1 & 2 \end{bmatrix} u_r \end{cases}$$

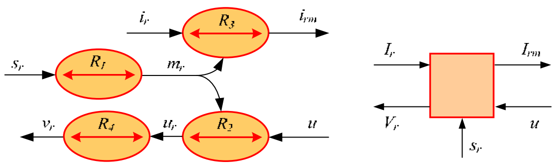

  - Grid side converter

$$\begin{cases} R_5:\ m_g = \begin{bmatrix} 1 & 0 & -1 \\ 0 & 1 & -1 \end{bmatrix} s_g \\ R_6:\ u_t = m_g u \\ R_7:\ i_{gm} = m_g{}^T i_t \\ R_8:\ v_t = \frac{1}{3}\begin{bmatrix} 2 & -1 \\ -1 & 2 \end{bmatrix} u_t \end{cases}$$

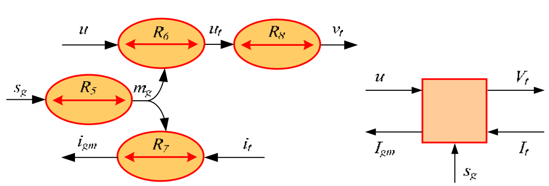

- Modeling of the DC bus

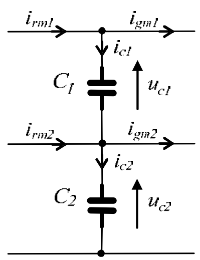

$$\begin{cases} R_9:\ C_1 \frac{du_{c1}}{dt} = i_{c1} \\ R_{10}:\ C_2 \frac{du_{c2}}{dt} = i_{c2} \\ R_{11}:\ i_{c1} = i_{rm1} - i_{gm1} \\ R_{12}:\ i_{c2} = i_{rm2} + i_{c1} - i_{gm2} \end{cases}$$

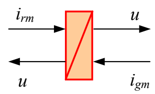

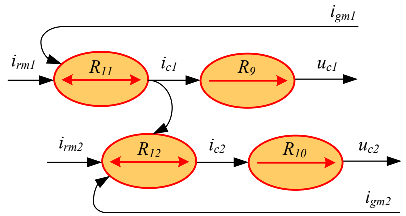

- Macroscopic representation of the system model with the control scheme

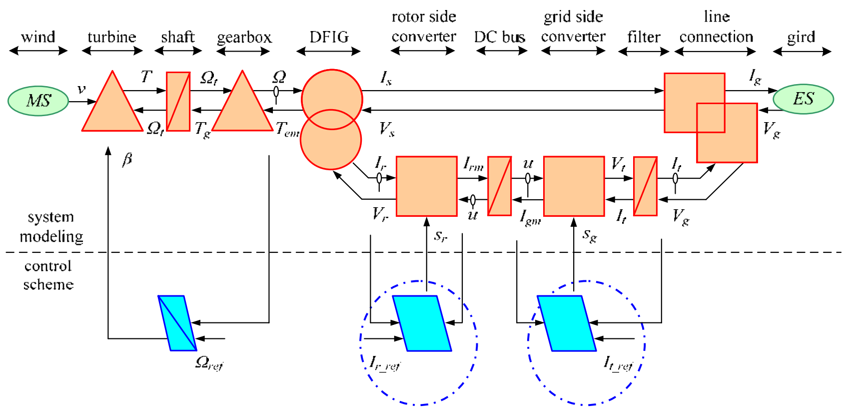

- Space-Vector Hysteresis Current Control

- Space-Vector Hysteresis Current Control
  - Simplicity
  - Outstanding robustness
  - Lack of tracking errors
  - Independence of load parameter changes
  - Extremely good dynamics
  - Reduced switching frequency
  - High usage of DC bus

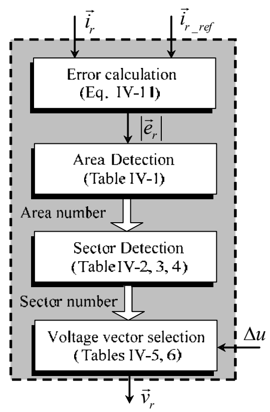

- Space-Vector Hysteresis Current Control
  - Current error vector is defined in α-β reference

$$\vec{e}_r = \vec{i}_r - \vec{i}_{r\_ref} = \vec{e}_{r\alpha} + j\vec{e}_{r\beta}$$

  - Current error vector tip location

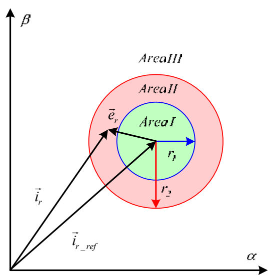

Three possible areas

Condition	Area
$\lvert\vec{e}_r\rvert < r_1$	Area I
$r_1 < \lvert\vec{e}_r\rvert < r_2$	Area II
$\lvert\vec{e}_r\rvert > r_2$	Area III

- Space-Vector Hysteresis Current Control
  - Angle between the error vector and the parallel to α axis

$$\theta = \arctan\left(\frac{\lvert\vec{e}_{r\beta}\rvert}{\lvert\vec{e}_{r\alpha}\rvert}\right)$$

  - Current error vector tip location

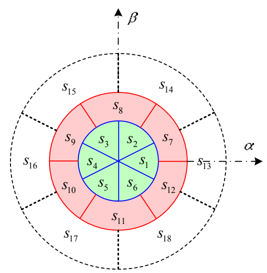

Eighteen possible sectors

Angle θ	Secteur
$-30° < \theta < 30°$	s_1
$30° < \theta < 90°$	s_2
$90° < \theta < 150°$	s_3
$150° < \theta < 210°$	s_4
$210° < \theta < 270°$	s_5
$270° < \theta < 330°$	s_6

- Space-Vector Hysteresis Current Control
  - Three-level converter voltage vectors

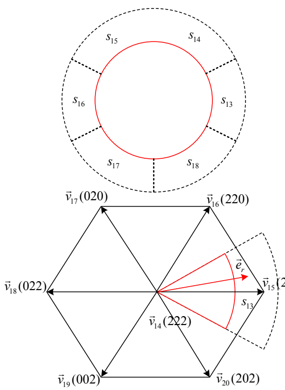

Area III：large hexagons

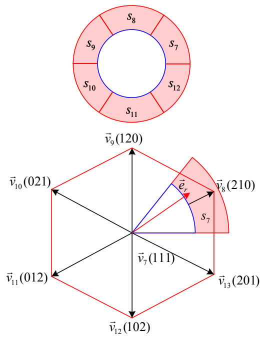

Area II：medium hexagons

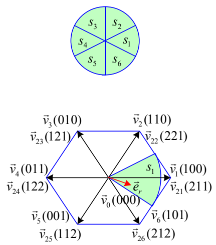

Area I：Small hexagons

- Space-Vector Hysteresis Current Control
  - DC-link voltage balancing algorithm

voltage vector	i_o	C_1 state	voltage vector	i_o	C_1 state	voltage vector	i_o	C_1 state
$\vec{v}_8(210)$	i_b	charging	$\vec{v}_1(100)$	i_a	charging	$\vec{v}_{21}(211)$	$-i_a$	discharging
$\vec{v}_9(120)$	i_a	charging	$\vec{v}_2(110)$	i_c	charging	$\vec{v}_{22}(221)$	$-i_c$	discharging
$\vec{v}_{10}(021)$	i_c	charging	$\vec{v}_3(010)$	i_b	charging	$\vec{v}_{23}(121)$	$-i_b$	discharging
$\vec{v}_{11}(012)$	i_b	charging	$\vec{v}_4(011)$	i_a	charging	$\vec{v}_{24}(122)$	$-i_a$	discharging
$\vec{v}_{12}(102)$	i_a	charging	$\vec{v}_5(001)$	i_c	charging	$\vec{v}_{25}(112)$	$-i_c$	discharging
$\vec{v}_{13}(201)$	i_c	charging	$\vec{v}_6(101)$	i_b	charging	$\vec{v}_{26}(212)$	$-i_b$	discharging

- Space-Vector Hysteresis Current Control
  - Selection of the appropriate voltage vector

	s1	s2	s3	s4	s5	s6
△u >0	$\vec{v}_{24}$	$\vec{v}_{25}$	$\vec{v}_{26}$	$\vec{v}_{21}$	$\vec{v}_{22}$	$\vec{v}_{23}$
△u <0	$\vec{v}_4$	$\vec{v}_5$	$\vec{v}_6$	$\vec{v}_1$	$\vec{v}_2$	$\vec{v}_3$

$\Delta u = u_{c1} - u_{c2}$

s7	s8	s9	s10	s11	s12
$\vec{v}_{11}$	$\vec{v}_{12}$	$\vec{v}_{13}$	$\vec{v}_8$	$\vec{v}_9$	$\vec{v}_{10}$
s13	s14	s15	s16	s17	s18
$\vec{v}_{18}$	$\vec{v}_{19}$	$\vec{v}_{20}$	$\vec{v}_{15}$	$\vec{v}_{16}$	$\vec{v}_{17}$

  - Zero voltage vectors are selected to minimize the switching frequency

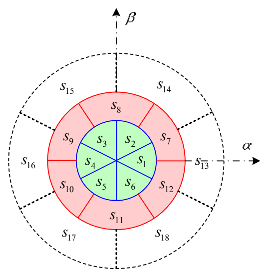

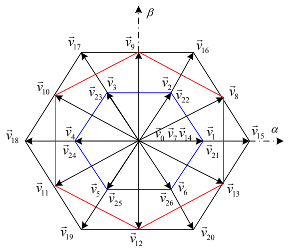

- Simulation results (500ms 50 % voltage dip)

- stator voltage

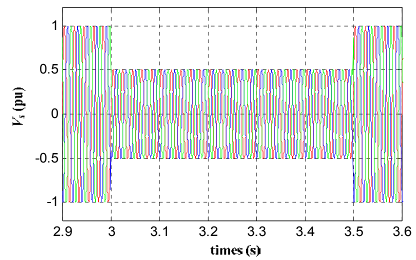

- rotor current

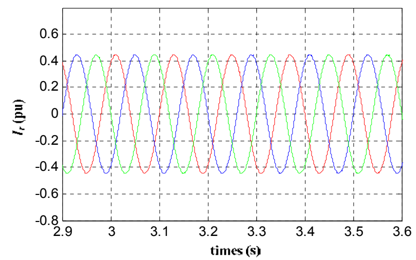

- Simulation results (500ms 50 % voltage dip)

• stator current

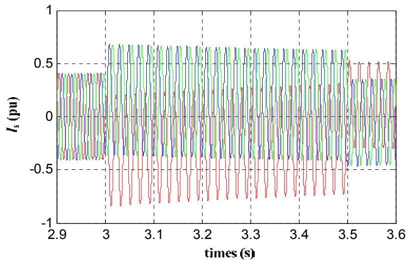

• DC-link voltage

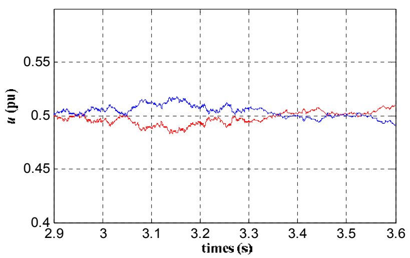

- Reconfiguration of control strategies
  - Hierarchical control structure

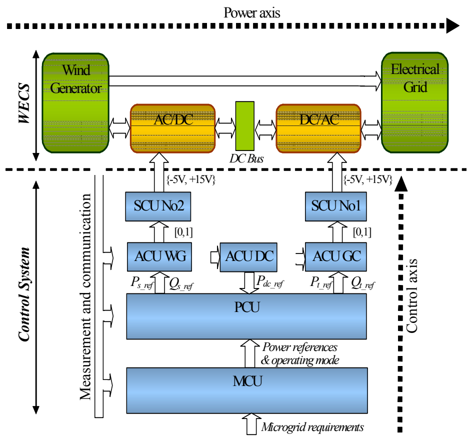

- Switching Control Unit (SCU)
- Automatic Control Unit (ACU)
- Power Control Unit (PCU)
- Mode Control Unit (MCU)

- Reconfiguration of control strategies
  - Hierarchical control structure

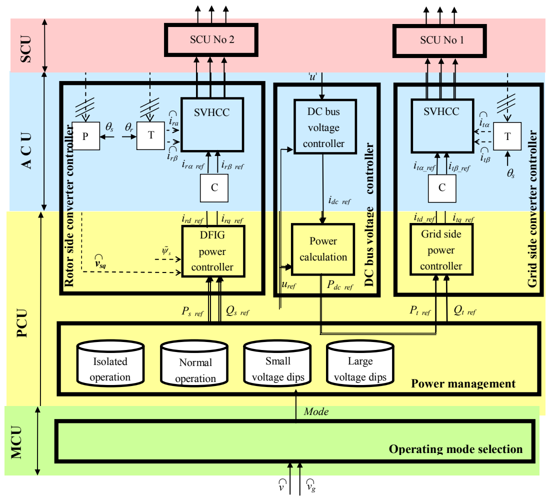

- Switching Control Unit (SCU)
- Automatic Control Unit (ACU)
- Power Control Unit (PCU)
- Mode Control Unit (MCU)

- Reconfiguration of control strategies

Isolated operation

- Synchronization

$$i_{rd\_ref} = i_{ms} = \frac{\psi_{sd\_ref}}{M}$$

$$i_{rq\_ref} = 0$$

Normal operation

- Torque control

$$i_{rq\_ref} = -\frac{1}{p\psi_{sd\_ref}}\frac{L_s}{M}T_{em\_ref} \ .$$

$$i_{rd\_ref} = \frac{\psi_{sd\_ref}}{M} - \frac{L_s}{v_{s\_ref}M}Q_{s\_ref} \ .$$

Small voltage dips

- Small voltage dips
  - Short duration

    i_{rd_ref}, i_{rq_ref} unchanged

  - Long duration

    $i_{rd\_ref} = \sqrt{\hat{i}^2_{r\_max} - \hat{i}^2_{rq}}$. grid support

    i_{rq_ref} unchanged

Large voltage dips

- Large voltage dips
  - Synthetic protection scheme using active crowbar

Experimental results of synchronization

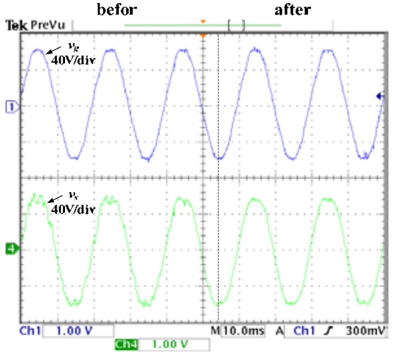

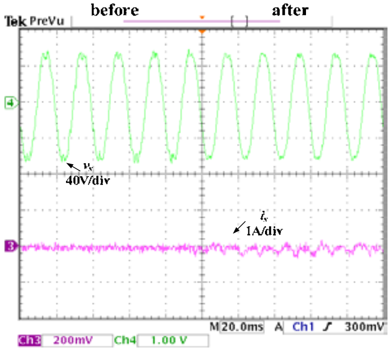

Static experimental results in normal operation mode

- stator current
- rotor current

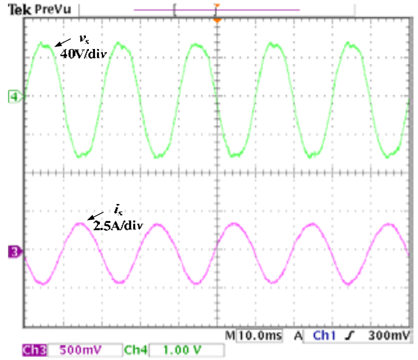

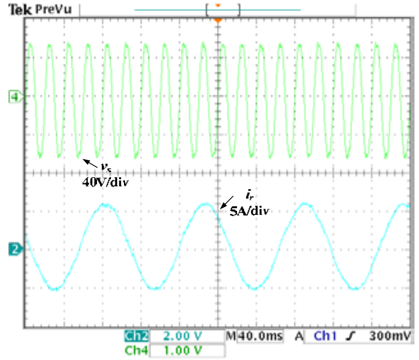

Dynamic experimental results in normal operation mode

- reactive power change
- active power change

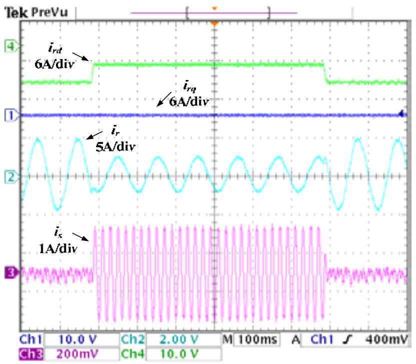

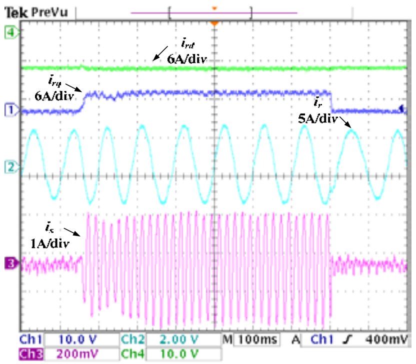

Comparison of experimental results during a grid voltage dip

- without reconfiguration
- with reconfiguration

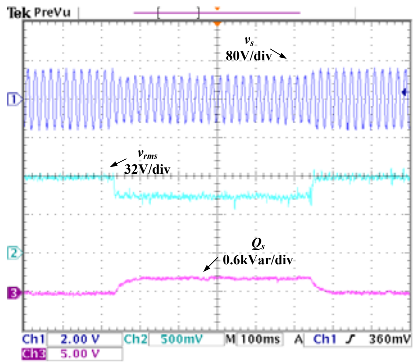

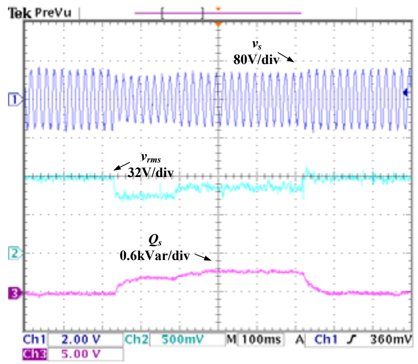

Control strategy of high power DFIG system

- Comparison of experimental results during a grid voltage dip

  - without reconfiguration

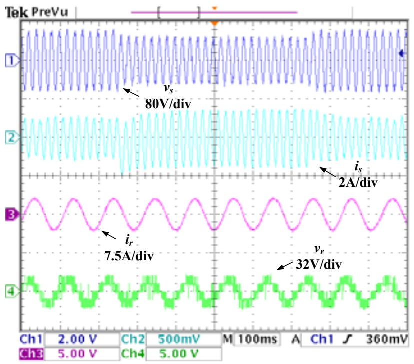

  - with reconfiguration

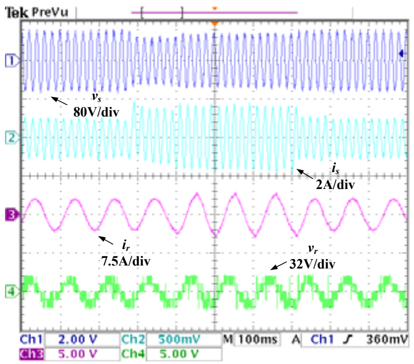

Tsinghua University

Outline

Tsinghua University

Conclusion

- The studied wind turbine system has been modeled with the help of COG and EMR. Then the control strategies have been deduced by using inversion rules, which show excellent performance of the system during normal grid condition.

- A modified vector control strategy of the DFIG has been proposed to provide adequate control of the generator during small voltage dips. It takes the dynamics of the stator flux into account, and can reduce the rotor over-current effectively.

- When the dip is too large, active crowbar has been implemented to protect the system. A hysteresis control strategy has been proposed to reduce the activated time, cooperated with demagnetization method and voltage support in order to improve the LVRT ability of the system.

Tsinghua University

Conclusion

- A Space-Vector Hysteresis Current Controller has been proposed to control the NPC converter of high power DFIG system, in order to improve the dynamic response. In this way, the rotor current can be controlled in a safe range during small voltage dips.

- A reconfiguration scheme of control strategies for the system has been proposed to meet the grid code requirements. With this specific methodology, the DFIG can provide active power in proportion to the retained voltage, while supplying maximum reactive current to the grid without exceeding generator limit during a long voltage dip.

Perspective

- The proposed control strategies should be further carried out on MW range practical DFIG wind turbine system in order to verify the controllability and the effectiveness.
- The obtained model can be extended to the integrated model of a wind farm, and then connected to the transmission network for further simulation studies to know how severe the voltage dip could be at the PCC.
- As the unsymmetrical grid faults are more common and it is more difficult to control the DFIG during asymmetrical voltage dips, the unsymmetrical fault ride-through strategies is worth researching.

Thanks for your attention！